ARMY RESEARCH LABORATORY

Characterizing the Turbulent Wind Flow Near a Wind Barrier Using a Data Set Collected with an Array of Sonic Anemometers

by Yansen Wang, David Tofsted, Jimmy Yarbrough, David Quintis, Robert Brice, Sean D'Arcy, Scott Elliott, Thomas Truong, and Michael Davalos

ARL-TR-4834 **May 2009**

NOTICES

Disclaimers

The findings in this report are not to be construed as an official Department of the Army position unless so designated by other authorized documents.

Citation of manufacturer's or trade names does not constitute an official endorsement or approval of the use thereof.

Destroy this report when it is no longer needed. Do not return it to the originator.

Army Research Laboratory
Adelphi, MD 20783-1197

ARL-TR-4834 **May 2009**

Characterizing the Turbulent Wind Flow Near a Wind Barrier Using a Data Set Collected with an Array of Sonic Anemometers

Yansen Wang, David Tofsted, Jimmy Yarbrough, David Quintis, Robert Brice, Sean D'Arcy, and Scott Elliott
Computational and Informational Sciences Directorate, ARL

and

Thomas Truong and Michael Davalos
Holloman High Speed Test Track, Holloman Air Force Base

REPORT DOCUMENTATION PAGE

Form Approved
OMB No. 0704-0188

1. REPORT DATE *(DD-MM-YYYY)*	2. REPORT TYPE	3. DATES COVERED (From - To)
May 2009	Final	

4. TITLE AND SUBTITLE

Characterizing the Turbulent Wind Flow Near a Wind Barrier Using a Data Set Collected with an Array of Sonic Anemometers

5a. CONTRACT NUMBER

5b. GRANT NUMBER

5c. PROGRAM ELEMENT NUMBER

6. AUTHOR(S)

Yansen Wang, David Tofsted, Jimmy Yarbrough, David Quintis, Robert Brice, Sean D'Arcy, Scott Elliott, Thomas Truong, and Michael Davalos

5d. PROJECT NUMBER

5e. TASK NUMBER

5f. WORK UNIT NUMBER

7. PERFORMING ORGANIZATION NAME(S) AND ADDRESS(ES)

U.S. Army Research Laboratory
ATTN: AMSRD-ARL-CI-ED
2800 Powder Mill Road
Adelphi, MD 20783-1197

8. PERFORMING ORGANIZATION REPORT NUMBER

ARL-TR-4834

9. SPONSORING/MONITORING AGENCY NAME(S) AND ADDRESS(ES)

10. SPONSOR/MONITOR'S ACRONYM(S)

11. SPONSOR/MONITOR'S REPORT NUMBER(S)

12. DISTRIBUTION/AVAILABILITY STATEMENT

Approved for public release; distribution unlimited.

13. SUPPLEMENTARY NOTES

14. ABSTRACT

An array of 10 sonic anemometers was used to observe the mean wind and turbulence near an artificial wind barrier at the High Speed Test Track facility on Holloman Air Force Base, NM. In order to test the effectiveness of such barriers in reducing cross-track winds, a prototype barrier was constructed using a polyester screen material rated as providing 30% porosity. The barrier dimensions were 100 m in length and 5 m in height. Turbulent wind data, with 20 Hz sampling frequency, were collected continuously over a four-day period using 10 sonic anemometers arranged in an array across the middle of the wind barrier. This report reviews literature related to this research and test, and describes the experimental design of the wind barrier and instrumentation. The document also reports on the analysis method and preliminary results of the mean wind and turbulent characteristics at the leeside of the wind barrier. The influences of wind direction and the atmospheric surface layer stability condition on the barrier effectiveness are also investigated. The report provides some suggestions on possible improvements for a future full-scale wind barrier construction based on the field test results.

15. SUBJECT TERMS

Turbulence, wind, wind barrier

16. SECURITY CLASSIFICATION OF:			17. LIMITATION OF ABSTRACT	18. NUMBER OF PAGES	19a. NAME OF RESPONSIBLE PERSON
a. REPORT	b. ABSTRACT	c. THIS PAGE			Yansen Wang
Unclassified	Unclassified	Unclassified	UU	28	19b. TELEPHONE NUMBER (*Include area code*) (301) 394-1310

Standard Form 298 (Rev. 8/98)
Prescribed by ANSI Std. Z39.18

Contents

List of Figures

List of Tables

Acknowledgments

We would like to thank Dr. Dennis Garvey and Mr. Robert Brown of the U.S. Army Research Laboratory for their helpful comments. The support of Holloman High Speed Test Track at Holloman Air Force Base, NM, is also acknowledged.

INTENTIONALLY LEFT BLANK.

1. Introduction

The Holloman High Speed Test Track (HHSTT) facility at Holloman Air Force Base (HAFB), NM, has a test section of 1.8 km that contains an artificial rain field generation capability over the track. The rain drops produced can be excessively deflected when the cross-track wind speed is greater than 1 m/s. To extend testing times to days when moderate wind conditions (1 to 5 m/s) are present, the HHSTT plans to construct a wind barrier for cross-track wind reduction. Before the construction of a complete wind barrier, an observational study was carried out by the U.S. Army Research Laboratory (ARL) and HHSTT personnel to characterize the mean and turbulent wind fields using a small prototype section of the wind barrier. This document reports the experimental design, instrumentation used, and the initial statistical analysis method used to process the observational data. The results not only provide important bases for the design and construction of full-scale wind barriers, but also are a valuable addition to the knowledge base in developing future computer models of microscale wind flows.

Wind barriers are widely applied to modify the flow field and other meteorological factors in the nearby area. The shelter effect of a wind barrier has been recognized for many years. Wind breaks or shelterbelts using either tall vegetative stands or artificial materials have been widely applied in agriculture practices and wind erosion control. Several observational studies (Heisler and DeWalle, 1988; Brandley and Mulhearn, 1983; Argete and Wilson, 1989; Nord, 1991) have reported wind speed reductions at the lee side of shelterbelts for various barrier porosities and wind directions. The wind speeds measured at the lee side of a barrier of height (H) were usually expressed as a percentage of undisturbed upwind velocity. Maximum wind speed reductions ranged from 60% to 80% of their undisturbed upwind speeds for moderate barriers with porosity ranging between 0.3 and 0.4. The location of the maximum reduction was commonly reported as between 3H and 5H away from the lee side of barrier depending on the barrier's porosity. Wind tunnel simulations (Woodruff and Zingg, 1953; Horn et al., 1971; Raine and Stevenson, 1977) indicated that porous wind barriers have better leeward sheltering effects in terms of sheltered area and overall speed reduction. Momentum absorption by the barrier's form and friction drag produces a region of mean wind speed reduction spanning roughly from –5H windward to 30H leeward. In addition to speed reductions, wind flows are deflected by the barrier, causing a faster flow jet above the barrier under high wind conditions. The turbulence due to the stronger shear of the jet increases in the barrier wake region except in its immediate lee. Numerical simulations (Plate, 1971; Wilson, 1985, 2004b; Wang and Takle, 1995) were able to reproduce the observed data from field and wind tunnel studies. The shelter effect of the wind barrier is not only dependent on wind direction relative to the barrier, the porosity of the barrier, and the thickness of the barrier, but also on the atmospheric boundary layer stability conditions present.

Although many references report field observational results for vegetative wind barriers and wind tunnel tests of very short obstacles, field test reports on artificial wind barriers are scarce (Bradley and Mulhearn, 1983; Wilson 2004a). Moreover, for the literature available, there are shortcomings in available data for the leeward wind field observational results: First, field tests on artificial wind barriers have generally focused on short barriers of 1- to 1.5-m height, not up to the height HHSTT required. Second, the materials and porosities of the wind barriers studied were quite different from the wind screen that HHSTT planned to use. And third, the sensors available in those studies provided only a sparse array. Therefore, the results from those studies are probably not directly applicable for the HHSTT wind barrier without drastic extrapolation. Other observational studies from vegetation wind barriers (shelterbelts) were even further removed in characteristics from the present setup and materials. The test performed was to evaluate the wind barrier at the site using a full-scale height to avoid the inaccuracies that would have resulted when extrapolating from these referenced former studies. This field test also accumulates the data sets for the tall, artificial wind barrier in different atmospheric stability categories and for different classes of wind oblique angle relative to a normal vector to the barrier's surface.

2. Wind Barrier Setup and Instrumentations

HHSTT is located northeast of the White Sands National Monument, NM, in a wide valley between the Sacramento Mountains approximately 15 mi to the east and the San Andres Mountains approximately 25 mi to the west of the track. The Hay Draw is a shallow arroyo 5–7 m deep and 60–70 m wide that runs from the east out of the Sacramento Mountains and passes directly beneath the track at around the 7 km point. Otherwise, the terrain is fairly flat with a gentle grade sloping from east towards the west. The track is oriented south to north with a slight (~5°) deflection from southeast to northwest direction in azimuth. The entire track is about 16 km long and a middle section (1.8 km) has artificial precipitation generation capability. Although the Hay Draw is less than 1 km to the south of this section, the width of the draw, its depth, and the distance to the track section under study combined to produce a minimal impact, as the fetch conditions would be reestablished prior to the wind flow field encountering the barrier fence. Along the track there is a nearly flat swath with a width of 400 to 500 m, the test cross-section elevation change from west to east is less than 1 m. The track itself is about 0.9 m above the ground surface, and the width of track is 2.2 m at the test section. The semi-desert land is mostly covered with sparse, short (<40 cm) desert bushes and shrubs.

A prototype wind barrier (figure 1a) with a length of 100 m and a height of 5 m was erected by HHSTT personnel parallel to the track at a distance of 20 m from the west side of the track. An observational tower and tripods array (figure 1b and 1c) were set up by ARL personnel perpendicular to and across the barrier fence line and test track at the midpoint of the barrier. A

6-m reference tower was located 30 m to the west of the wind barrier, with two UVW RM Young 81000 sonic anemometers located at 2-m and 6-m heights. Mounting booms were used to separate the anemometers to a distance of approximately 1.5 m from the center of the tower. Booms were mounted to point south, into the direction of the expected flow.

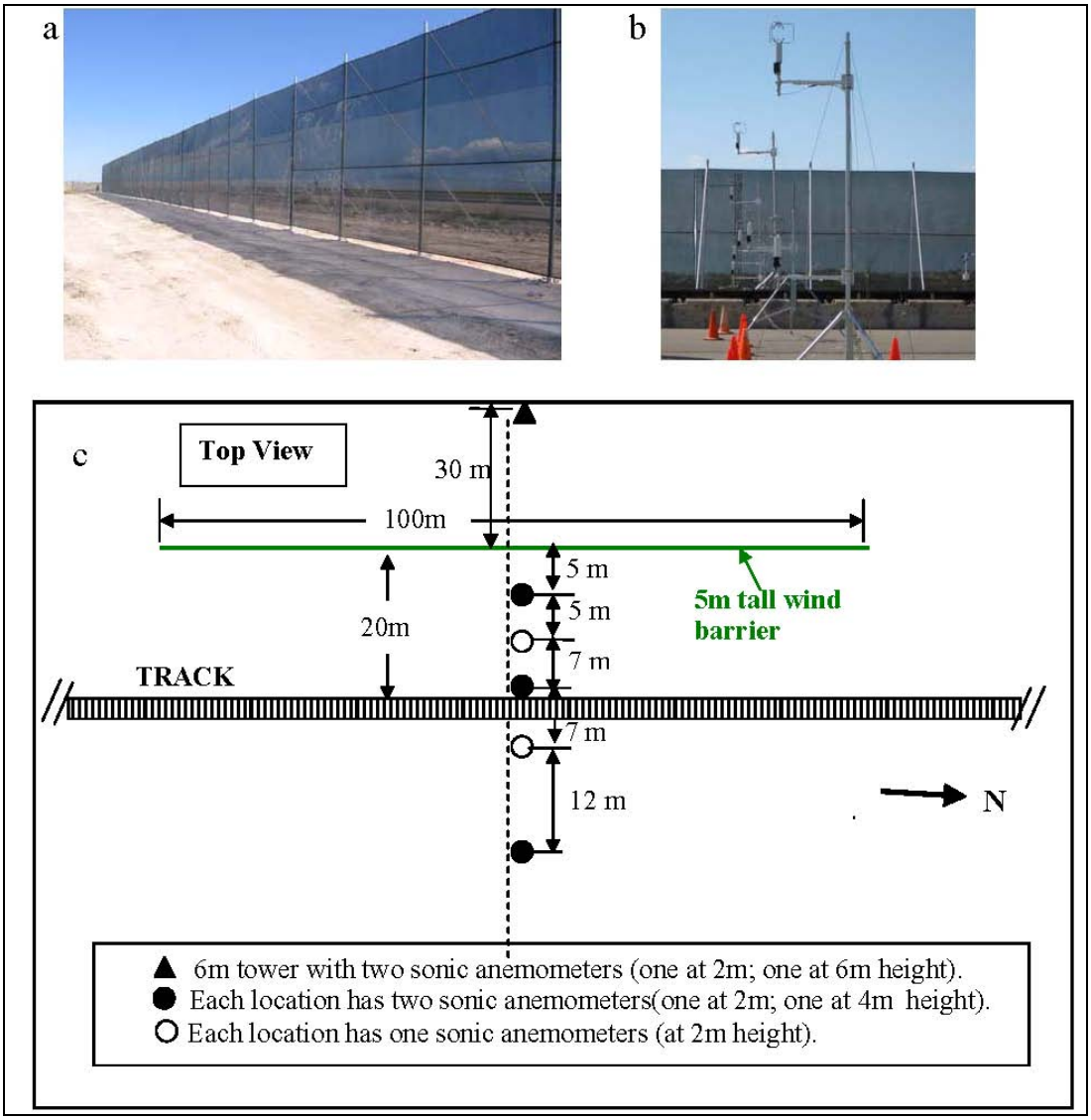

Figure 1. The wind barrier set up and sonic anemometers arrangement. (a) A wind barrier photography taken near the southwest corner of the barrier. (b) A photograph showing the sonic anemometer arrangement across the wind barrier, taken on the east side of the wind barrier looking west. (c) A schematic diagram showing the wind barrier, anemometer placements, and track location.

Five additional tripods, with eight additional sonic anemometers, were located to the east of the wind barrier (see figure 1c), using alternating anemometer arrangements; three tripods with two sonic anemometers were set up at distances of 5 m, 17 m, and 36 m from the barrier; and two tripods with one sonic anemometer were set up at distances of 10 m and 24 m from the barrier. Each of these tripods had a 2-m anemometer attached at the end of a 1-m boom extension, while

the three tripods had an additional sensor at 4-m height. The sonic anemometers were oriented such that their V axis was parallel to the track and wind barrier for the convenience of instrumentation setup and data analysis. The sampling time for all instruments was synchronized with a sampling frequency of 20 Hz. The data were collected on two laptop computers running the Linux operating system (OS). The data were collected continuously over the observational period and were stored hourly for each instrument. Data files for each instrument were coded according to their instrument position relative to the tower plus the hour and date of collection for ease of use in post-test data processing. The observations period was from 1600 Mountain daylight time (MDT), 18 September 2008, to 1400 MDT, 22 September 2008.

The wind barrier material was purchased from Midwest Cover of Griffith, IN. The screen material for the wind break consists of a vinyl-coated polyester, also known as PermaScreen 70, which has 30% porosity. An image of a sample of the wind screen material is shown in figure 2. We have used the magnified image to estimate the porosity, confirming the validity of the 30% value. The screen material was tightly attached, using a series of metal clips, to an array of metal poles with additional metal strut reinforcements (figure 1a.). Besides the porosity of the screen material, its arrangement and the size of the holes might be a significant factor for the flow near the wind barrier; therefore, a note of caution regarding extrapolation of these observational results in comparison with measurements of other types of wind barrier materials must be raised here.

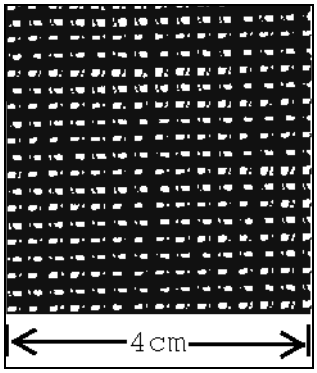

Figure 2. Image of a sample of the wind screen material with 30% porosity used for the wind barrier.

3. Data Analysis and Results

3.1 Mean Wind Speed Profile Without Barrier Effect

The atmosphere near the ground is termed the surface layer and is governed by the surface roughness, and the momentum and heat fluxes at the ground surface. Over a fairly flat and homogenous ground and stationary conditions, the mean wind and temperature profiles follow

the Monin-Obukhov similarity theory (MOST). This theory is based on an assumption of local equilibrium of turbulence production and dissipation; therefore, it is ideal for uniform or near uniform terrains. MOST states that wind and temperature profiles are parameterized using the scaling parameters, u_*, T_*, and z/L, defined as

$$u_* = \left\{ \left[\overline{(u'w')}_0 \right]^2 + \left[\overline{(v'w')}_0 \right]^2 \right\}^{1/4} \tag{1}$$

$$T_* = -\overline{(w'\theta')}_0 / u_* \tag{2}$$

$$\frac{z}{L} = \frac{kzgT_*}{\theta_0 u_*^{\,2}} \tag{3}$$

where superscript primes represent turbulent fluctuations, over-bars denote averaged turbulent fluxes, subscript 0 denotes fluxes at the surface, k is von Karman's constant, z is the height, θ is the potential temperature, and L is the Monin-Obukhov (MO) length.

The ratio z/L is the surface layer atmospheric stability parameter. The resulting similarity profile for wind is as follows (Businger et al., 1971; Dyer, 1974):

$$\phi_m(z/L) = (kz/u_*)(\partial u/\partial z) \tag{4}$$

where ϕ_m is the non-dimensional momentum function. Integration of equation 4 results in the following stability-modified logarithmic wind profile:

$$U(z) = \frac{u_*}{k}\left[\ln(z/z_0) - \psi_m\right] \tag{5}$$

where z_0 is the roughness length of the ground surface, k is von Karman's constant (~0.4), and ψ_m is the integral of $(1 - \phi_m)/(z/L)$ over limits of z_0/L to z/L. For neutral atmospheric condition, the value is zero. Kaimal and Finnigian (1994) have listed the ψ_m values with respect to different ranges of the stability condition parameter, z/L.

It is important to use the collected test data to determine whether MOST can be applied to conditions observed at HHSTT. The validated results can give us confidence to use similarity profiles to parameterize the undisturbed ambient flow when a single point observation is used to initialize the model. From analysis of many profiles, it is indicated that the roughness length z_0 at this site lies somewhere in the range of 3 to 7 cm. Therefore, a roughness length value of 5 cm was used throughout the analysis for this test site. Figure 3 shows an example of a logarithmic wind profile fitted to a particular case of fetch tower winds using the estimated roughness length of 5 cm, and using analyzed friction velocity and stability parameter ψ_m computed at 6 m.

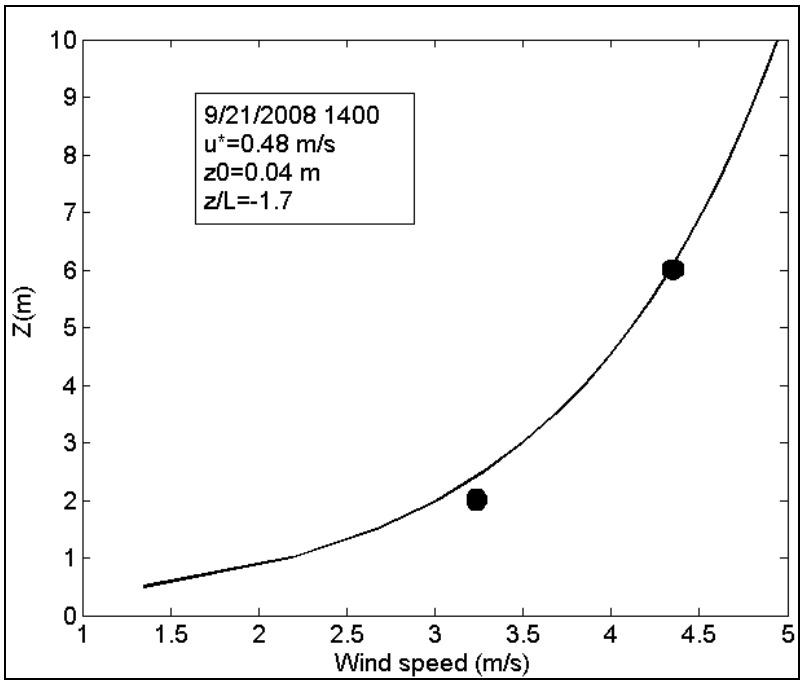

Figure 3. An example of logarithmic wind profile derived from the u*, z0, and L.

The roughness length is actually dependent on stability conditions as well (Kaimal and Finnnigan, 1994). It is our hope that we find a reasonable estimate of the stability parameter ψ_m through our analysis. The logarithmic wind profile is very sensitive to the choice of roughness length. It is unfortunate we did not have enough observations under the neutral conditions with strong winds to better estimate the roughness length. The estimate of roughness length would be more reliable with the availability of such data.

3.2 Cross-track Wind Component at Leeward Side of the Wind Barrier

This test is to characterize the average behavior of turbulent winds in the vicinity of a wind barrier. In order to achieve the objective, the continuous data sections used for analysis must be quasi-stationary in terms of wind speed and direction. Unlike controlled laboratory data collections such as in wind tunnel experiments, non-stationary winds are prevalent in atmospheric boundary layer flows and are functions of the wind speed, ground surface morphology, and atmospheric stability conditions. One technique to treat such non-stationary conditions is to sample the data, section by section, according to certain stationarity criteria. First, the mean wind speed has to be greater than 1 m/s, for the reason that the wind barrier has very little effect at very low wind speeds. Second, the variance of the horizontal wind angle must be less than 10°. Third, the time span of any given stationary section must be at least 5 min long in order for the incoming wind flow to establish a roughly uniform pattern throughout the entire 80-m-long horizontal domain where the anemometers are located.

Based on these sampling criteria, data sections were categorized according to the wind speed and direction relative to the wind barrier and the atmospheric stability condition. Due to the placement of the leeward instruments on the east side of the wind barrier, the ambient wind must be upwind from the west side of the barrier where the reference tower was located. During the period of the data collections, most of the winds directed from the south or southwest occurred during the daytime hours, meaning the atmosphere was primarily unstable for most of the applicable cases for analyzing the barrier leeside winds. Table 1 lists the 5-min samples used for the following analysis, where the wind obliquity angle provided the primary classification factor.

Table 1. Number of 5-min sample sections used for the analysis for different wind oblique angle (angle from line perpendicular to wind barrier).

Wind oblique angles (°)	0–5	5–10	10–15	15–20	20–25	25–30	30–35
Number of 5-min. samples	4	6	12	9	18	10	16
Wind oblique angles (°)	35–40	40–45	45–50	50–55	55–60	60–65	65–70
Number of 5-min. samples	23	27	26	31	32	29	27

For the application at HHSTT, the most important characteristic of the wind barrier is its cross-track wind reduction capability. Most reported observational studies have neglected to discriminate between perpendicular and along barrier wind components because the total wind was the primary interest in most agricultural and other applications. One might have expected the cross-track wind reduction to be related to the obliquity angle (defined as the amount the incident wind angle is deviated from the perpendicular to the wind barrier). Figure 4 shows the bin-averaged results of 5-min data sets arranged according to the obliquity angle to the barrier. The data analysis revealed some quite unexpected characteristics of the cross-track wind reduction. First, the cross-track components of the wind had very small dependence on the wind direction at the leeside of the barrier. Secondly, the reductions in the cross-track winds are much greater than expected. At the 2-m height (figure 4a), the cross-track wind component showed a slight flow reversal with a very small amplitude (less than 10% of the reference total wind). As for the cross-track wind component reduction, the wind barrier effectiveness extended to at least 7H in the horizontal direction on the leeside, corresponding to the furthest anemometer position. Even for the 4-m height, the cross-track wind reduction was very significant. As indicated, the prototype wind barrier is very effective for the cross-track wind reduction even for large incident oblique angles to the wind barrier.

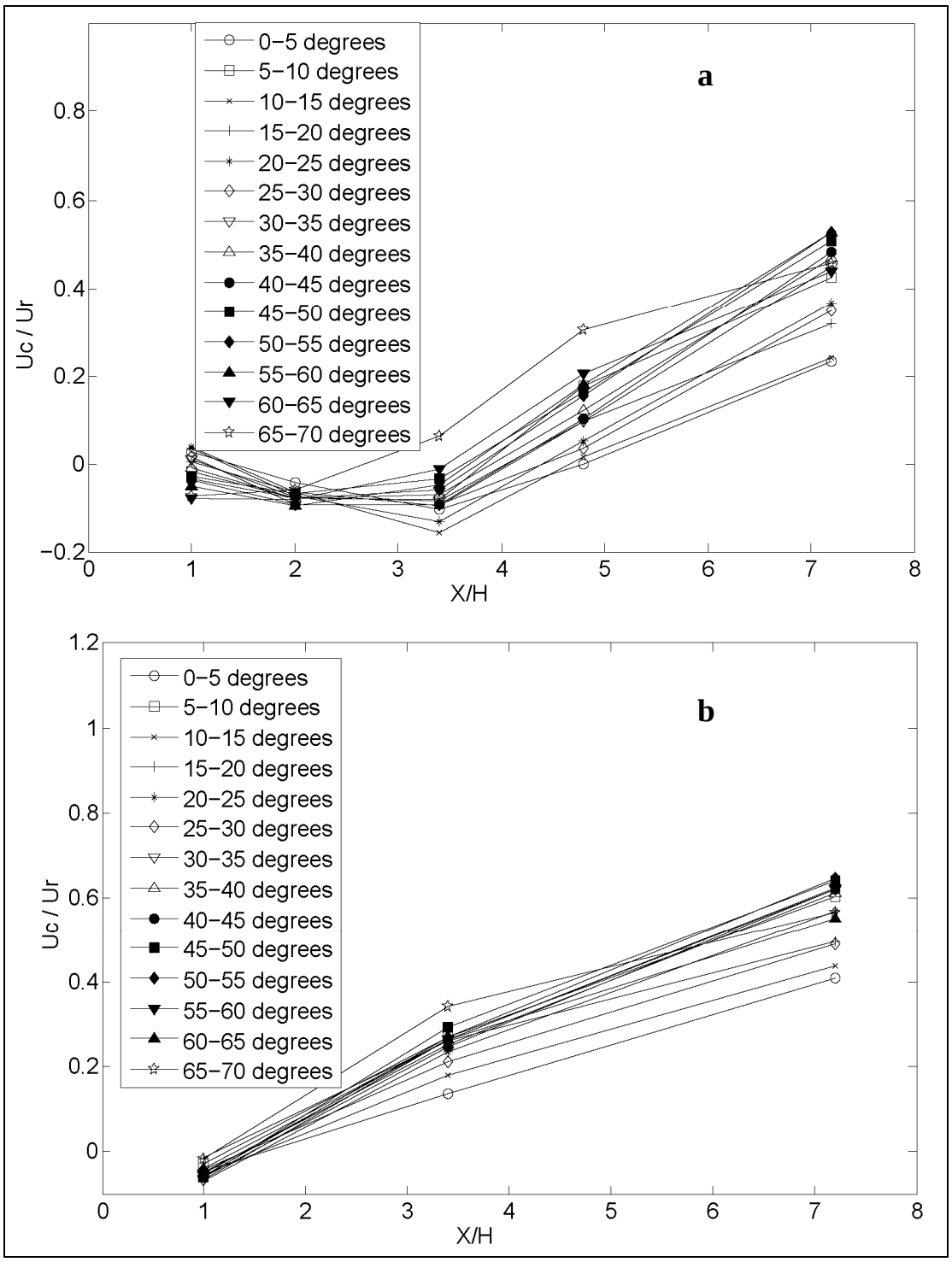

Figure 4. Averages of cross-track wind components (Uc) at (a) 2-m and (b) 4-m heights. The cross-track winds are scaled relative to the total mean wind speed measured by the reference tower's 2-m anemometer (Ur). The data are displayed according to the degrees difference between the mean wind direction and the direction perpendicular to the wind barrier (the oblique angle). The horizontal distance from the barrier is normalized by the barrier height (H). The wind barrier is at 0H location.

3.3 Mean Wind Reduction at Leeside of the Wind Barrier

For many applications of wind barriers, such as crop/animal protection or reduction of wind erosion effects, the mean total wind reduction is an important characteristic. In order to compare with these former studies, we considered the reduction in the total wind speed as a function of distance from the wind barrier, height above ground, and angle of attack. Wind barriers are most effective when the wind direction is perpendicular to the barrier in terms of the mean wind reduction. This reduction decreases as the obliquity angle increases. During the four days of data collection, wind directions were rarely exactly perpendicular to the wind barrier (table 1). Wind direction, even within half hour time periods, varied significantly depending on several factors such as mean wind speed and atmospheric stability conditions. However, the dominant feature appeared to be the obliquity angle relative to the barrier normal. For this reason, we subdivided the data into several the wind direction angle classes according to obliqueness of the wind direction with respect to the barrier.

Figure 5 shows the mean wind speed perpendicular to the wind barrier, the mean total wind speed (defined as $U = (u^2 + v^2 + w^2)^{1/2}$) measured is scaled relative to the 2-m anemometer wind speed measured at the reference tower. For winds at 2 m above the ground (figure 4a), the cross-track wind component showed reductions up to 90% at distances up to 5H beyond the barrier, when the wind blows through the wind barrier. Oblique winds at angles of 5° to 15° showed reductions of around 70% up to 5H from the barrier. The mean wind shelter effect gradually reduced as the oblique angle increased. The wind barrier lost its effectiveness on the mean wind reduction when the wind obliquity angle reached 40°. The mean wind reduction at the 4-m height (figure 4b) followed a similar pattern as that at the 2-m height. The effective sheltering distance, however, reduced from 5H to 3H, and the mean wind reduction was less than that at the 2-m height, especially for large oblique angles.

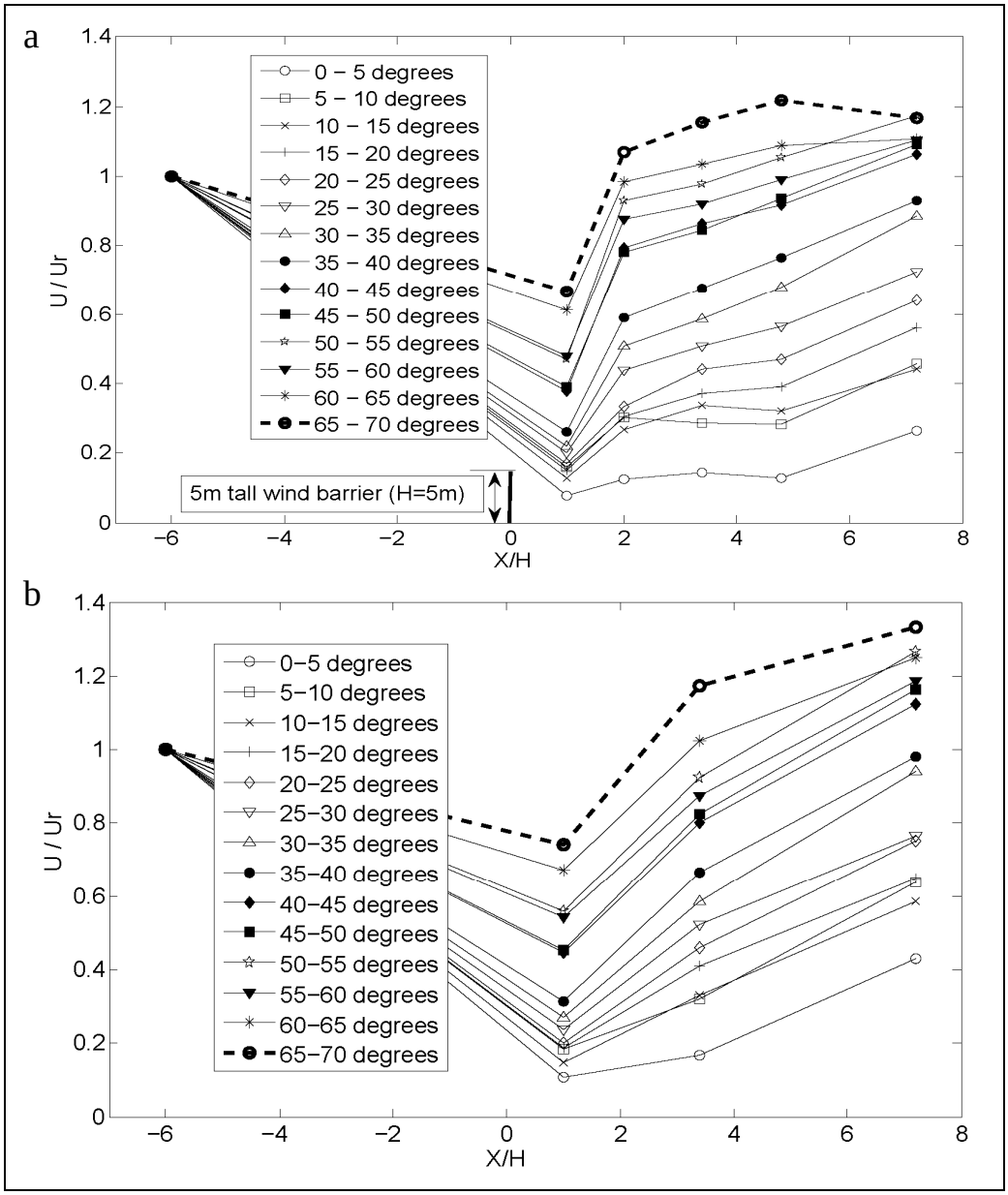

Figure 5. Averages of total wind speed (U) at the (a) 2-m height and (b) 4-m height, scaled by the total wind speed of the 2-m reference anemometer (Ur). The degrees are the oblique angles from the perpendicular to the wind barrier. The wind barrier is at 0H location.

3.4 Mean Wind Angular Deflections at the Leeward Side of the Wind Barrier

From the discussions in sections 3.2 and 3.3, cross-track wind reductions are much more significant than reductions in total winds because wind direction at the leeside of the barrier had a fairly large change compared with the reference approaching wind vector. There are very few reports on this aspect of the wind barrier effect. Figure 6 shows an averaged space-time series of the section data. For comparison with the undisturbed approaching wind, averaged wind vectors are shown for each sonic anemometer except the one at the 6-m height at the reference tower.

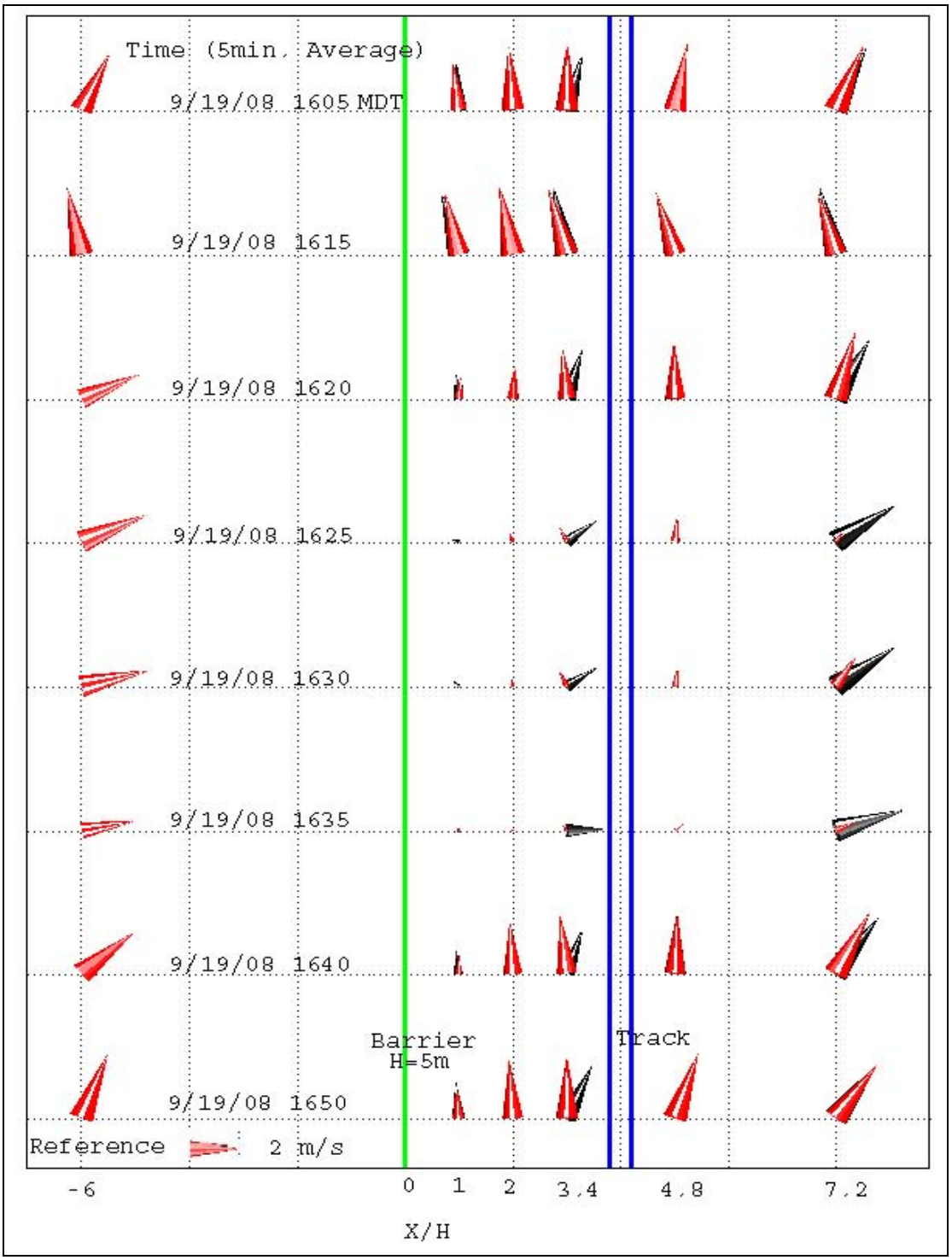

Figure 6. A space-time plot of 5-min averaged wind vectors at each anemometer location. Black arrows represent the wind vectors at the 4-m heights; red arrows represent wind vectors at the 2-m heights; the green line denotes the wind barrier; and the blue parallel line represents the track location.

Several points can be derived from figure 6. First, the wind at the 4-m height showed smaller wind directional changes from the reference wind than for the winds measured by the 2-m anemometers. Second, wind directions are rotated almost parallel to the wind barrier at distances up to the 5H separation tripod. Although the total wind speed showed small reductions when the oblique angle was greater than 40°, the wind direction was altered to almost parallel to the barrier at the leeside of the barrier. This property definitely is a benefit to the HHSTT cross wind reduction objective. In other words, the wind barrier is effective in reducing cross-track winds even when the wind has a large oblique angle with respect to the track. With 30% porosity and the screen design used, the wind direction also shows a reversal behavior near the barrier when the wind is nearly perpendicular to the barrier. As displayed in figures 4 and 5, the mean wind reduction is most effective when the wind is nearly perpendicular to the wind barrier. The numerical simulation indicated that the wind direction change at the leeside of the barrier is due to a combination of the pressure gradient force and the turbulent transport of momentum (Wang and Takle, 1995).

3.5 The Wind Barrier Effect and the Influence of Surface Layer Stability Conditions

The state of atmospheric stability is an important factor in determining how effective the barrier will be in reducing winds on the leeward side of the barrier. During the daytime and under low wind speed conditions, surface heating causes many large scale thermal plumes. Under such conditions, there will be moderate upward vertical (~1 m/s) motion in the cores of thermal plumes and there will be a small general subsidence in the remaining volume of the daytime mixed layer in between these plumes. The artificial wind barrier constructed mainly absorbs horizontal momentum via form and friction drag effects. Therefore, under unstable, weak wind speed conditions, the wind barrier's effects will be reduced. Figure 7 shows the mean wind reduction under different stability conditions as a function of the MO length scale. Since we were not able to collect sufficient data under different stability conditions where the wind obliquity angle was nearly perpendicular to the barrier (0–5° oblique angle), a mean wind direction of 15–20° obliquity angle was used for comparison purposes. The wind speeds in these samples were all between 1.5 and 2 m/s, except for the two highly unstable samples (L = –1.17, –0.56) where they were below 1 m/s. Nevertheless, these limited data samples show that in the slightly stable or neutral conditions (L = 2.49, 6.63, and –1.39), the wind barrier had 80% wind reduction up to 5H, while the mean wind reduction quickly vanishes under highly unstable, low wind speed conditions

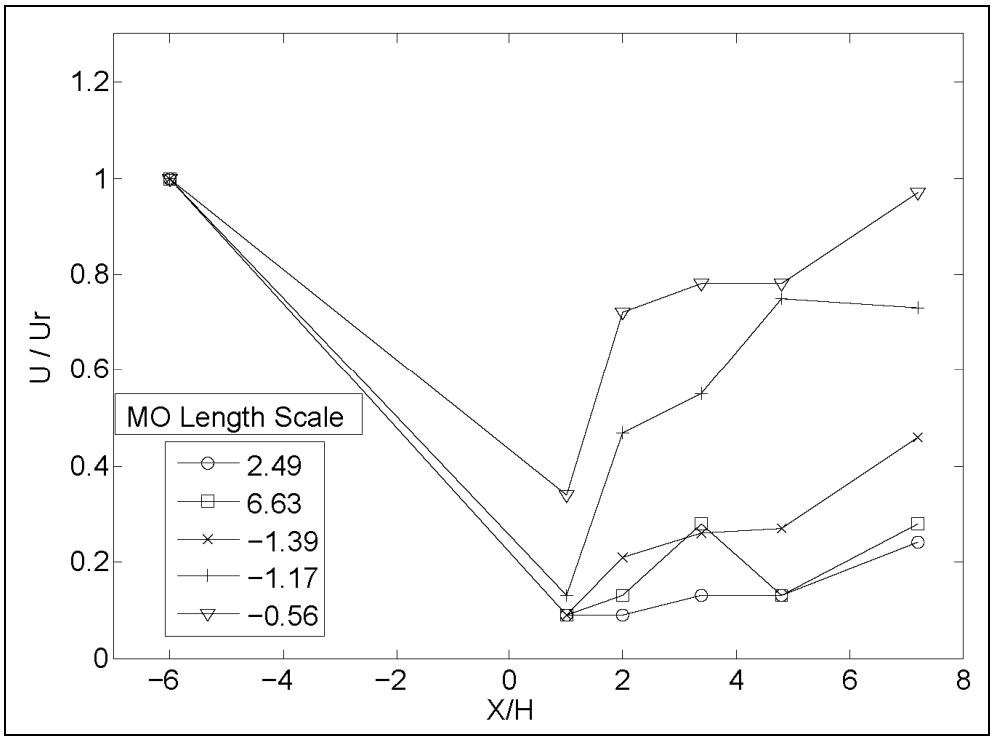

Figure 7. Averages of total wind speed under different atmospheric stability conditions. Positive MO lengths represent stable conditions; negative MO lengths represent unstable conditions.

3.6 Turbulence Characteristics in the Vicinity of Wind Barrier

The presence of the wind barrier also has an impact on the magnitude of the mechanical turbulence observed in the vicinity of the barrier, as well as on the turbulent transport of momentum and scalar atmospheric properties (humidity, temperature, etc.) past the barrier. Few field observations of turbulent characteristics in the vicinity of a wind barrier have been reported (Bradley and Mulhearn, 1983; Wilson, 2004a) due to the limitations of older anemometers and data collection equipment. With the use of highly accurate sonic anemometers and computer software able to collect data at sampling rates of 20 Hz in this observational study, the turbulent characteristics near the wind barrier were well characterized.

Figure 8 shows the turbulent kinetic energy (*TKE*) to the leeside of the wind barrier as a function of downwind distance. The *TKE* is defined as follows by averaging the instantaneous turbulent kinetic energy:

$$TKE = \frac{1}{2}\left(\overline{u'^2} + \overline{v'^2} + \overline{w'^2}\right) \tag{6}$$

The *TKE* statistics indicate the turbulence was reduced on the leeward side of the wind barrier up to 2H to 3H compared with the *TKE* sensed by the reference anemometer, which would contain no barrier effects. Beyond 3H, the *TKE* values increase by about 20% to 40% with respect to the

reference values. This *TKE* response is virtually independent of the wind obliquity angle. This result is largely in agreement with the observational results reported by other researchers (Bradley and Mulhearn, 1983; Wilson 2004a). The barrier effect on the turbulence intensities is another important factor for the wind barrier design. We should not only consider the reduction of cross-track and total wind, but also the turbulence intensities for the reason that increased mechanical turbulence tends to randomize the raindrop trajectory pattern, resulting in a less accurate simulation of actual rain conditions.

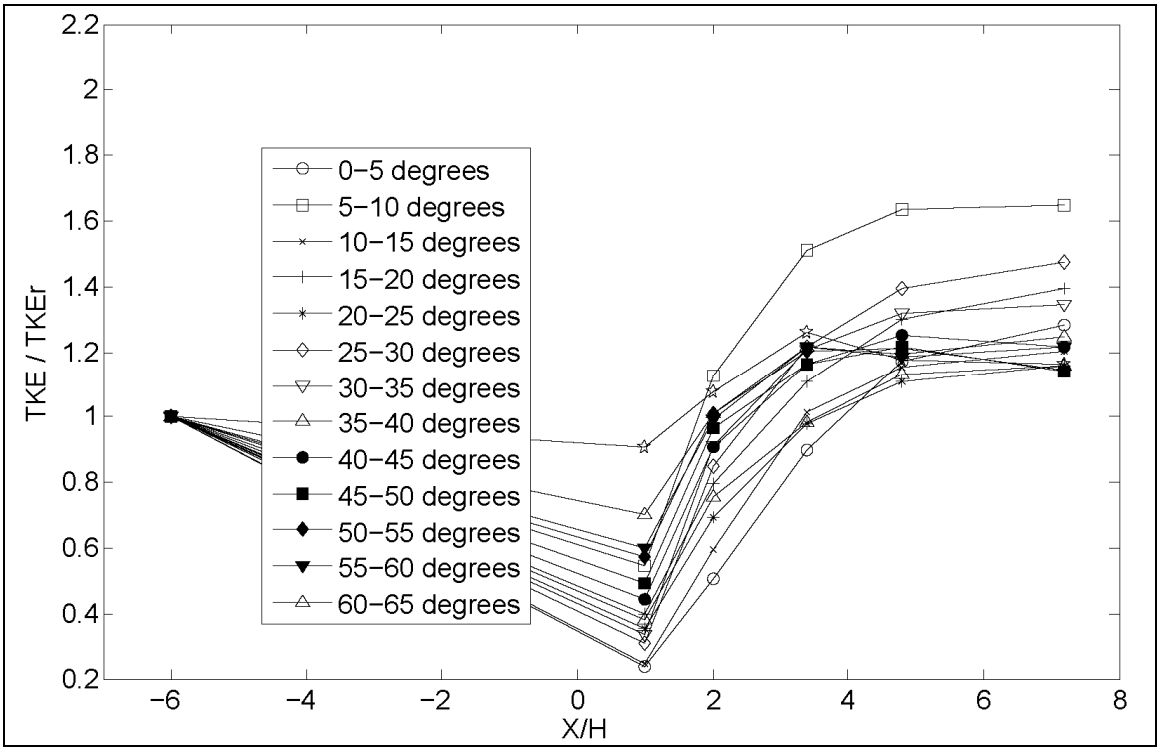

Figure 8. Shows the averaged *TKE* computed from the 5-min data sets at the 2-m height.

4. Conclusions

This report documents experimental design and instrumental arrangements for a wind barrier test at HHSTT, NM. Field observations indicated that the wind barrier with 5-m height and oriented parallel to the test track is very effective in reducing the cross-track wind component, even with large oblique angles of wind. The 2-m cross-track wind speed component (where the rain drops start) was greatly reduced: to 10% of the total wind speed of the undisturbed reference. The total wind speed at the leeward side of the barrier, however, is very much dependent on the wind oblique angle. The wind barrier lost its efficacy for total wind speed reductions when the wind angle became greater than 35–40° relative to the barrier normal vector. This observation was in agreement with results reported from earlier observational studies. The wind direction

experiences a large rotation at the leeward side of the wind barrier when the wind is not perpendicular to the barrier. The wind direction tends to orient more parallel to the barrier upon encountering the barrier. The atmospheric stability condition has significant influence on the barrier efficacy. The wind reduction by the barrier diminishes when the surface layer is highly unstable and wind speed is lower than 1 m/s. The 2-m height *TKE* at 3H to 4H to the leeside of the barrier is smaller than at the reference point, but the *TKE* is larger beyond this range and at 4-m height.

5. Recommendations

The following are suggestions for improved wind barrier construction:

1. *The porosity.* The barrier screen material used in this test is a reasonably good choice. Since the hole size is small and uniform on the screen, it tends to reduce the mean wind a little more than we expected from previous studies. It also appears that the wind direction rotates more at the leeside when the wind is not perpendicular to the barrier than when using a higher porosity material. This is property that will be beneficial to the HHSTT objective of reducing the cross-track wind.

2. *The barrier location.* The optimal horizontal distance is about 3H (15 m) toward the windward side of the test track, since the wind speed reaches a minimum at this range (figure 4) for a porosity of 0.3. This horizontal spacing between the barrier and the track will also reduce undesirable operational interference. The turbulence analysis indicated that *TKE* is reduced up to 3H before it reaches values equal or greater than that at the reference anemometer. As an alternative to moving the barrier position, one could also raise the barrier height to 7 m, thereby increasing the coverage distance to 21 m.

3. *Wind angle relative to the barrier.* The wind barrier remains effective in reducing the cross-track wind even when the wind oblique angle is highly oblique and as large as 70°, but the wind barrier loses its efficacy in reducing the total wind when the oblique angle reaches 40°.

4. *The height of the wind barrier.* The height of 5 m is reasonable compromise for reducing the mean and cross-track wind at a 2-m height. Any wind barrier with height less than 5 m will be not adequate.

5. *Barrier length.* The barrier at the two end points should have extensions of 20 to 30 m from the first and last rain sprayer in order to increase the efficacy of crosswind reductions at higher obliquity angles and increase the area of coverage for smaller angles. At the end

points of the wind barrier, the wind speed is slightly greater than the approach wind. The strong horizontal mixing will reduce the shelter effect of the barrier near the end points, so the extension is needed.

6. *Possible wind barriers at both sides of the track.* It is desirable to have wind barriers at both sides of the track if the prevailing wind is from the east on a significant percentage of days. This modification would provide useful reductions in crosswinds from both the west and east directions.

6. References

Argete, J. C.; Wilson, J. D. The Microclimate in the Centre of Small Square Sheltered Plots. *Agric. For. Meteor.* **1989**, *48*, 185–199.

Bradley, E. F.; Mulhearn, P. J. Development of Velocity and Shear Stress Distributions in the Wake of a Porous Shelter Fence. *J. Wind Eng. Ind. Aerodyn.* **1983**, *15*, 145–156.

Businger, J. A.; Wyngaard, J. C.; Ixumi, Y.; Bradley, E. F. Flux-Profile Relationships in the Atmospheric Surface Layer. *J. Atmos. Sci.* **1971**, *28*, 181–189.

Dyer, A. J. A Review of Flux-profile Relationships. *Boundary-Layer Meteorol*. **1974**, *7*, 363–372.

Heisler, G. M.; Dewalle, D. R. Effects of Windbreak Structure on Wind Flow. *Agric. Ecosyst. Environ.* **1988**, *22/23*, 41–69.

Horn, J. D.; Campbell, G. S.; Wallis, A. L.; McIntyre, R. G. Wind Tunnel Simulation and Prototype Studies of Barrier Flow Phenomena. U.S. Army Electronic Command: Fort Monmouth, NJ, 1971.

Hoidale, M. M.; Gee, B. J.; Harm, G. W. Atmospheric Structure, White Sands Missile Range, New Mexico, Part I, Surface Wind, Cloud Cover, Visibility. ECOM-5202, Atmospheric Sciences Laboratory. U.S. Army Electronics Command: White Sands Missile Range, NM, 1968.

Kaimal, J. C.; Finnigan, J. J. *Atmospheric Boundary Layer Flows;* Oxford University Press, 289, 1994.

Monin, A. S.; Obukhov, A. M. Basic Laws of Turbulent Mixing in the Ground Layer of the Atmosphere. *Trans, Geophys. Inst. Akad. Nauk USSR*, **1954**, *151*, 163–187.

Nord, M. Shelter Effects of Vegetation Belts—Results of Field Measurements. *Bound.-Layer Meteor.* **1991**, *54*, 363–385.

Plate, E. J. The Aerodynamics of Shelter Belts. *Agri. Meteorol.* **1971**, *8*, 203–222.

Raine, J. K.; Stevenson, D. C. Wind Protection by Model Fences in a Simulated Atmospheric Boundary Layer. *J. Indust. Aerodyn*. **1977**, *2*, 159–180.

Wang, H.; Takle, E. S. A Numerical Simulation of Boundary-Layer Flows Near Shelterbelts. *Boundary-Layer Meteorol.* **1995**, *75*, 141–173.

Wang, H.; Takle, E. S. Momentum Budget and shelter Mechanism of Boundary-layer Flow Near a Shelterbelt. *Bound.-Layer Meteor.* **1997**, *82*, 417–435.

Wilson, J. D. Numerical Studies of Flow Through a Windbreak. *J. Wind Eng. Ind. Aerodyn.* **1985**, *21***,** 119–154.

Wilson, J. D. Oblique, Stratified Wind about a Shelter Fence. Part I: Measurements. *J. App. Meteorol*. **2004a**, *43*, 1149–1167.

Wilson, J. D. Oblique Stratified Wind about a Shelter Fence. Part II: Comparison of Measurements with Numerical Models. *J. App. Meteorol.* **2004b**, *43*, 1392–1409.

Woodruff, N. P.; Zingg, A. W. Wind Tunnel Studies of Shelterbelt Models. *J. Forest* **1953**, *53*, 171–178.

List of Symbols, Abbreviations, and Acronyms

ARL	U.S. Army Research Laboratory
H	height
HAFB	Holloman Air Force Base
HHSTT	Holloman High Speed Test Track
MO	Monin-Obukhov
MOST	Monin-Obukhov similarity theory
TKE	turbulent kinetic energy

NO. OF COPIES	ORGANIZATION
1 ELEC	ADMNSTR DEFNS TECHL INFO CTR ATTN DTIC OCP 8725 JOHN J KINGMAN RD STE 0944 FT BELVOIR VA 22060-6218
1 HC	DARPA ATTN IXO S WELBY 3701 N FAIRFAX DR ARLINGTON VA 22203-1714
1 CD	OFC OF THE SECY OF DEFNS ATTN ODDRE (R&AT) THE PENTAGON WASHINGTON DC 20301-3080
1 HC	US ARMY RSRCH DEV AND ENGRG CMND ARMAMENT RSRCH DEV AND ENGRG CTR ARMAMENT ENGRG AND TECHNLGY CTR ATTN AMSRD AAR AEF T J MATTS BLDG 305 ABERDEEN PROVING GROUND MD 21005-5001
1 HC	PM TIMS, PROFILER (MMS-P) AN/TMQ-52 ATTN B GRIFFIES BUILDING 563 FT MONMOUTH NJ 07703
1 HC	US ARMY INFO SYS ENGRG CMND ATTN AMSEL IE TD F JENIA FT HUACHUCA AZ 85613-5300
1 HC	COMMANDER US ARMY RDECOM ATTN AMSRD AMR W C MCCORKLE 5400 FOWLER RD REDSTONE ARSENAL AL 35898-5000
2 HCs	HOLLOMAN HIGH SPEED TEST TRACK ATTN M DAVALOS ATTN T TRUONG HOLLOMAN AFB NM 88330
1 HC	US GOVERNMENT PRINT OFF DEPOSITORY RECEIVING SECTION ATTN MAIL STOP IDAD J TATE 732 NORTH CAPITOL ST NW WASHINGTON DC 20402
1 HC	US ARMY RSRCH LAB ATTN AMSRD ARL CI OK TP T LANDFRIED BLDG 4600 ABERDEEN PROVING GROUND MD 21005-5066
1 HC	DIRECTOR US ARMY RSRCH LAB ATTN AMSRD ARL RO EV W D BACH PO BOX 12211 RESEARCH TRIANGLE PARK NC 27709
1 HC	US ARMY RSRCH LAB ATTN AMSRD ARL CI ED S D'ARCY BATTLEFIELD ENVIR DIV WHITE SANDS MISSILE RANGE NM 88002-5001
5 HCS	US ARMY RSRCH LAB ATTN AMSRD ARL CI ED R BRICE ATTN AMSRD ARL CI ED S ELLIOTT ATTN AMSRD ARL CI ED D QUINTIS ATTN AMSRD ARL CI ED D TOFSTED ATTN AMSRD ARL CI ED J YARBROUGH WSMR NM 88002-5501
4 HCs	US ARMY RSRCH LAB ATTN AMSRD ARL CI EM Y WANG ATTN AMSRD ARL CI OK PE TECHL PUB ATTN AMSRD ARL CI OK TL TECHL LIB ATTN IMNE ALC HRR MAIL & RECORDS MGMT ADELPHI MD 20783-1197
TOTAL:	22 (1 ELEC, 1 CD, 20 HCs)